

Second-order self-energy of the Hubbard Hamiltonian: Absence of quasiparticle excitations near half-filling

J. Galán and J. A. Vergés

*Instituto de Ciencia de Materiales de Madrid (Sede B), Consejo Superior de Investigaciones Científicas (C-XII),
Universidad Autónoma de Madrid, E-28049 Madrid, Spain*

A. Martín-Rodero

Departamento de Física de la Materia Condensada (C-XII), Universidad Autónoma de Madrid, E-28049 Madrid, Spain

(Received 22 July 1992; revised manuscript received 22 July 1993)

The electron self-energy $\Sigma(\mathbf{k}, \omega)$ corresponding to the one-band Hubbard Hamiltonian on clusters of the square lattice has been obtained as a function of the band filling up to second order in the interaction parameter U . The \mathbf{k} dependence of the self-energy is completely taken into account. As a consequence, the imaginary part of the self-energy shows a linear behavior for fillings close to one electron per site whereas for large doping rates the quadratic ω dependence characterizing Fermi liquids is recovered. The origin of this behavior has been investigated analytically: linear terms associated with nesting are shown to exist in any finite-dimensional lattice although its numerical relevance decreases very rapidly for space dimensionality larger than two. Implications of these results on the renormalization factor Z have been analyzed. From a practical point of view, we conclude that a standard second-order perturbative treatment is quantitatively precise for U values of the on-site Coulomb interaction smaller than the bandwidth of the noninteracting spectrum.

I. INTRODUCTION

Since the discovery of the high T_c superconductors,¹ there has been a renewed interest in strongly correlated systems. The simplest model proposed² to explain both the normal and the superconducting phases of this material taking into account the electron correlation is the one-band Hubbard Hamiltonian.³ Although it has been extensively studied by a great number of groups, very few exact results are presently known. Not only does the pairing mechanism remain a mystery but also the transport and spectral properties of the normal metallic state of this compound are not well understood.⁴

One phenomenological model that explains qualitatively most of the anomalous properties of the normal state is the marginal Fermi liquid hypothesis.⁵ A microscopical explanation for the rather drastic assumption made in this model about the low-temperature charge and spin polarizabilities has not yet been achieved. The basic assumption made in Ref. 5 can be summarized in the following behavior for the electron self-energy:

$$\Sigma(\mathbf{k}, \omega) \sim g^2 N^2(0) \left(\omega \ln \frac{x}{\omega_c} - i \frac{\pi}{2} x \right), \quad (1)$$

$$x = \max(|\omega|, T).$$

The most interesting characteristic of Eq. (1) is the linear behavior of the imaginary part of the self-energy close to the Fermi energy [$\text{Im}[\Sigma(\mathbf{k}, \omega)] \sim \omega$ for $\omega \sim 0$]. This linear dependence implies a logarithmic vanishing of the quasiparticle weight.

Several attempts have been made to derive this behav-

ior of the self-energy⁶⁻⁹ from first principles. In the work of Schweitzer and Czycholl⁶ the self-energy originated by the interaction term of the Hubbard Hamiltonian was obtained in standard second-order perturbation theory. Starting from the local approximation for $\Sigma(\mathbf{k}, \omega)$ (which is exact in an infinite-dimensional Hubbard model¹⁰), a $1/N$ expansion was developed in the half-filled case for the one-, two-, and three-dimensional models. The importance of considering the whole \mathbf{k} dependence in one and two dimensions was demonstrated. Also Moreo *et al.*¹¹ computed the second-order self-energy of an 8×8 cluster of the square lattice for $U/t = 4$ and half an electron per site. Their results were in excellent agreement with Monte Carlo simulation. On the other hand, Ref. 7 stressed the relevance of the nesting of the Fermi surface that occurs in the square lattice close to half-filling. Its relation to the nonconventional behavior of the self-energy was also addressed.

More generally, the second-order self-energy approximation to the Green function has been extensively used in many-body calculations¹² proving its usefulness to deal near the small interaction limit. Besides a previous work¹⁴ showed that a second-order perturbative analysis of the Hubbard Hamiltonian of the two-dimensional 4×4 cluster gave quantitative agreement with Monte Carlo simulations of the same system up to U values comparable to the bandwidth of the noninteracting case (a similar conclusion was reached in Ref. 15 studying the one-dimensional chain of six sites). In the present paper we extend the range of validity of the perturbative analysis through the computation of the second-order self-energy in clusters of different sizes and for the whole range of

fillings. Special attention is paid to the range of validity of the method and to the behavior of the imaginary part as a function of the number of holes added to the cluster. We leave for future work the computation of magnitudes that could be related with experiment within a realistic model including Cu-O planes (spin susceptibility, magnetic structure factor, or correlation functions, for example). Work in this line was done in Ref. 13. They successfully compared the weak coupling predictions [random phase approximation (RPA)] for the transverse nuclear relaxation rate and the magnetic response with experiments on $\text{YBa}_2\text{Cu}_3\text{O}_7$.

II. METHOD

The Hamilton operator representing the Hubbard model is

$$\hat{H} = -t \sum_{\langle ij \rangle, \sigma} \hat{c}_{i, \sigma}^\dagger \hat{c}_{j, \sigma} + U \sum_i \hat{n}_{i, \sigma} \hat{n}_{i, -\sigma} , \quad (2)$$

where $\hat{c}_{i, \sigma}^\dagger$ creates an electron of spin σ on site i , $\langle ij \rangle$ represent pairs of nearest-neighbor sites on the two-dimensional square lattice, $\hat{n}_{i, \sigma}$ is the electron occupation operator on site i and spin σ , $-t$ is the hopping energy ($t > 0$), and U is the on-site Coulomb interaction.

There are only two parameters in the model: first, U/t , which is a dimensionless ratio that measures the importance of the on-site Coulomb interaction relative to the hopping energy, and, second, the number of electrons per site that fill in the system. We will start from the small U/t limit and will later show that our results are valid up to U values comparable to the bandwidth W of the noninteracting case. As usual we will work in the grand canonical ensemble and control the number of electrons adding a chemical potential term $\mu_0 \hat{N}$ to the Hamilton operator given by Eq. (2).

The self-energy of the electrons is computed within perturbation theory up to second order. Standard rules at zero temperature¹⁶ give the following expression:

$$\Sigma_\sigma^{(2)}(\mathbf{k}, \omega) = U n_{-\sigma}^{(1)} + \left(\frac{U}{L}\right)^2 \sum_{\mathbf{p}, \mathbf{q}} \frac{\Theta(\epsilon_{\mathbf{k}+\mathbf{q}})\Theta(\epsilon_{\mathbf{p}-\mathbf{q}})[1 - \Theta(\epsilon_{\mathbf{p}})] + [1 - \Theta(\epsilon_{\mathbf{k}+\mathbf{q}})][1 - \Theta(\epsilon_{\mathbf{p}-\mathbf{q}})]\Theta(\epsilon_{\mathbf{p}})}{\omega - U n_{-\sigma}^{(1)} - \epsilon_{\mathbf{k}+\mathbf{q}} - \epsilon_{\mathbf{p}-\mathbf{q}} + \epsilon_{\mathbf{p}}} , \quad (3)$$

where L is the number of sites, Θ is the step function, $\epsilon_{\mathbf{k}}$ is the unperturbed dispersion relation, and $n_{-\sigma}^{(1)}$ is the Hartree occupation of spin $-\sigma$. As it is shown explicitly by the denominator of the second-order term, the Hartree solution is used as the starting point.

The double sum in momentum can be easily done for chain lengths up to 2000 sites in the one-dimensional model. Unfortunately, computational effort increases as the fourth power of the side of the cluster in the more interesting two-dimensional system. Nevertheless, one can save a lot of memory and time of computation taking into account that most of the terms in Eq. (3) have the same denominator and can be grouped in only one term after adding numerators. With this method we were able to study two-dimensional clusters up to 40×40 for some magnitudes. In the three-dimensional case the effort that is necessary to evaluate this summation increases even more rapidly as the cluster size increases. Therefore, it is more advantageous to follow the method described in Ref. 6 in this case.

The advantages of our approach are the following.

(i) It is a systematic and proven approximation to obtain the one-particle spectrum and related properties of the Hubbard Hamiltonian.^{14,15,17,18} We will show later that the present form of second-order perturbation theory yields accurate results within the range $U/t \leq W$. Most probably, this interaction regime applies to high- T_c compounds.¹⁹⁻²¹

(ii) Cluster sizes as large as 40×40 sites can be considered with a reasonable numerical effort. All the parameters appearing in the model such as the U value, system filling, or temperature can be easily changed, in

contrast with the limitation of size and temperature for exact diagonalizations and Monte Carlo.²⁴⁻²⁶

(iii) Effects related to the finite size of the cluster can be easily isolated increasing the number of sites of the cluster. We have checked that all results presented in this work have been converged to the corresponding continuous limits.

(iv) In principle, this approximation can be further improved adding families of diagrams of higher orders or considering a self-consistent solution for higher values of U/t .

Of course the limitations are also clear: We will never be able to study the large U/t limit within our perturbative scheme. In particular, the atomic limit of the Hubbard model will never be reached (upper and lower Hubbard bands). A second but minor limitation of our perturbative analysis is that we will never be able to study the *exactly* half-filled case, since in this case the Fermi level coincides with a highly degenerate one-electron level. This situation is not tractable within our method because levels should be either completely filled or completely empty in our calculations to avoid uncertainties in the evaluation of the noninteracting Green function. For example, we saw in our previous study¹⁴ that one has to use standard perturbation theory of degenerate levels to obtain the ground state of half-filled clusters. This is not a severe limitation because the half-filled limit is continuously approached as soon as the cluster size is increased. Moreover, we can do a scale analysis whenever it is necessary.

Using $\Sigma(\mathbf{k}, \omega)$ the following physical magnitudes can be directly calculated:

(i) *Energy:*

$$E = -\frac{i}{2} \lim_{\eta \rightarrow 0^+} \sum_{\mathbf{k}, \sigma} \int_{-\infty}^{\infty} \frac{d\omega}{2\pi} e^{i\omega\eta} [\omega + \epsilon_{\sigma}(\mathbf{k})] G^{\sigma}(\mathbf{k}, \omega), \quad (4)$$

where, as usual, η guarantees that the occupied poles of the Green function contribute to the integral.

(ii) *Number of electrons:*

$$N = -i \lim_{\eta \rightarrow 0^+} \sum_{\mathbf{k}, \sigma} \int_{-\infty}^{\infty} \frac{d\omega}{2\pi} e^{i\omega\eta} G^{\sigma}(\mathbf{k}, \omega). \quad (5)$$

At this point, it is worth mentioning that our solution verifies Luttinger theorem,²² i.e., there exists an energy that plays the role of the Fermi energy in the many-body system. Unfortunately, since $\Sigma(\mathbf{k}, \omega)$ is truly \mathbf{k} dependent, the shape of the interacting Fermi surface is different from the noninteracting one and the new Fermi energy is not easily related to the original one.

(iii) *Momentum distribution:*

$$\begin{aligned} n(\mathbf{k}) &= \left\langle \sum_{\sigma} c_{\mathbf{k}\sigma}^{\dagger} c_{\mathbf{k}\sigma} \right\rangle \\ &= -i \lim_{\eta \rightarrow 0^+} \sum_{\sigma} \int_{-\infty}^{\infty} \frac{d\omega}{2\pi} e^{i\omega\eta} G^{\sigma}(\mathbf{k}, \omega). \end{aligned} \quad (6)$$

In this work, we have always started perturbation theory from the paramagnetic ground state. This situation does not change after adding a finite number of perturbation diagrams to the noninteracting Green function. Therefore, both spin directions are equally populated in all of our solutions.

(iv) *Renormalization constant Z :*

$$Z = \left| 1 - \frac{\partial \text{Re} \Sigma(\mathbf{k}_F, \omega)}{\partial \omega} \right|_{\omega=\epsilon_F}^{-1}. \quad (7)$$

The possibility of calculating Z in this way depends critically on the good convergence of the real part of the self-energy to its continuous limit. In the next section, we will use these equations to evaluate the relevant magnitudes of chains and clusters of the square lattice.

III. RESULTS

We have checked our approach comparing the energy with results of the one-dimensional case²³ and small two-dimensional clusters: 4×4 , 8×8 , and $\sqrt{10} \times \sqrt{10}$, where precise numerical results are available.^{24–26} Let us begin with some results concerning the one-dimensional Hubbard model.

A. One-dimensional case

An analytic investigation of the one-dimensional case reveals several interesting features of the second-order self-energy. The analysis is based on the approximate linearization around the Fermi energy of all the dispersion relations that appear in Eq. (3). The validity of this

expansion is surprisingly large: of the order of magnitude of t as the comparison with numerical results shows a *posteriori*. In this way, it is possible to perform the single integral over momenta that remains in Eq. (3) when the imaginary part of the second-order self-energy is evaluated. Based on the perfect nesting that exists in one dimension for any filling factor, a *naive* reasoning shows that the allowed integration space increases as a linear function of $|\omega|$ giving

$$\text{Im} \Sigma_{\sigma}^{(2)}(k_F, \omega) = -\frac{U^2}{4\pi |d\epsilon_k/dk|_{k=k_F}^2} |\omega|. \quad (8)$$

Applying this result to the half-filled situation, the following nonanalytic behavior of the imaginary part of the self-energy is obtained:

$$\text{Im} \Sigma_{\sigma}^{(2)}\left(\frac{\pi}{2}, \omega\right) = -\frac{U^2}{16\pi t^2} |\omega|. \quad (9)$$

These results do not take into consideration possible divergences of the integrand. When they are properly considered, the numerical prefactor that appears in Eq. (9) diminishes somewhat:

$$\text{Im} \Sigma_{\sigma}^{(2)}\left(\frac{\pi}{2}, \omega\right) = -\frac{3U^2}{64\pi t^2} |\omega|. \quad (10)$$

An analysis of the behavior of the imaginary part of the self-energy that takes into account the divergences of the integrand shows that the *naive* result given by Eq. (8) is strictly valid for fillings smaller than one-quarter but should be corrected in other cases. Nevertheless, the appearance of a linear term in $|\omega|$ remains. Now, this analytic prediction can be compared with numerical results obtained for very long chains. The linear dependence on $|\omega|$ is confirmed by our calculation and besides we found that this behavior extends over a very large energy range (see Fig. 1 where the imaginary part of the self-energy is given for the Fermi wave vector). This last feature is related to a further property of $\text{Im} \Sigma_{\sigma}^{(2)}$: It can be proved that the imaginary part is an odd function of $|\omega|$. As a consequence, only odd powers of $|\omega|$ appear in a series expansion about the Fermi energy and the range of linear $|\omega|$ dependence increases.

The existence of two different energy scales should be emphasized. The first scale is related to the form variation of the Fermi surface as the perfect nesting situation is left behind. As soon as the Fermi surface is deformed, the volume argument that gives Eqs. (8) and (9) loses its validity. On the other hand, there is a second energy scale related to the correctness of the linearization of energy dispersion relations. As our numerical results show, this second energy scale is much larger than the first one and explains the linear behavior of the imaginary part of the self-energy well behind the nesting condition. This point is particularly relevant in the application of the second-order perturbation theory to the square lattice: While a linear ω dependence around the Fermi energy does not survive the change in occupation, the global

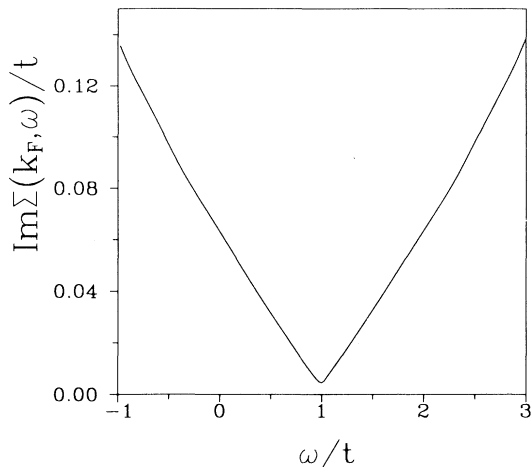


FIG. 1. Imaginary part of the second-order self-energy of a chain of 2000 sites calculated as a function of energy at the Fermi wave vector. We have used a small broadening to smooth the self-energy function. It is this small but finite broadening the only reason of the nonzero value of the imaginary part of the self-energy at the Fermi energy ($E_F = t$ for $U = 2t$).

linear behavior remains after large changes of the band filling (see Sec. III B).

Figure 2 shows the ground-state energy as a function of band filling for several U values. Perturbative results are compared with exact results obtained within the Bethe ansatz.²³ It can be seen that our second-order approach [Eq.(4)] works accurately up to $U = 4t$, i.e., while U is less than the bandwidth. Moreover, it can be observed that perturbation theory works better after separating the system from half-filling.

B. Square lattice

As mentioned above, we have first checked the range of applicability of our approach through a comparison with exact results obtained for small clusters of the square lattice. Figure 3 compares the ground-state energy ob-

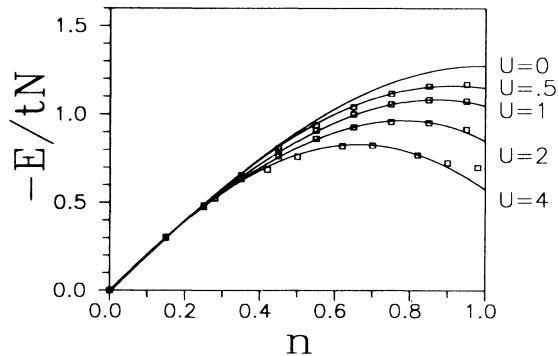


FIG. 2. Ground-state energy per site vs band filling of the one-dimensional Hubbard model plotted for several U values. The number of electrons per lattice site is n . Solid lines are exact results from Shiba (Ref. 23) whereas small squares are second-order results obtained by means of Eq. (4).

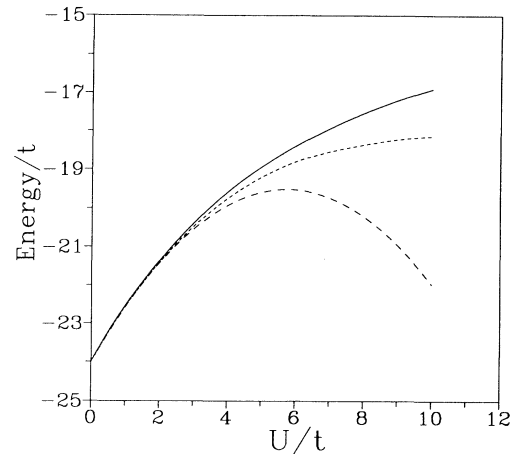


FIG. 3. Ground-state energy vs U for ten electrons on a 4×4 cluster of the square lattice. The solid line gives exact results obtained by the Lanczos method (Ref. 25), the dashed line gives *naive* second-order results of a previous calculation, and the dotted line gives present results obtained by Eq. (4).

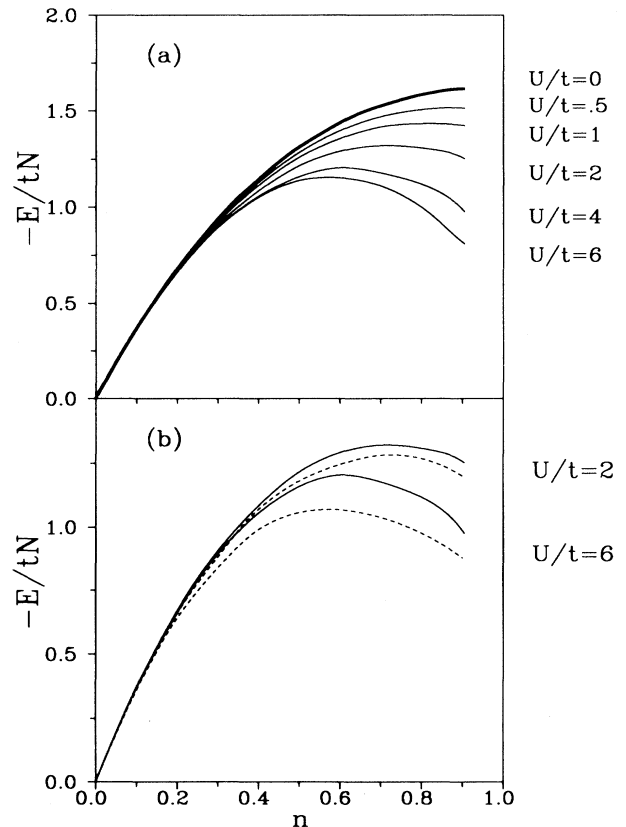


FIG. 4. Ground-state energy vs band filling of the two-dimensional Hubbard model for several U values. (a) Second-order results. (b) Comparison of second-order results with mean field solutions of the unrestricted Hartree Fock (Ref. 27) type (dashed lines).

tained via second-order perturbation theory with Lanczos results for the 4×4 cluster.²⁵ It can be seen that an accurate estimate of the energy is obtained up to U values comparable with the bandwidth ($8t$). In addition, we can learn by comparison with previous results obtained by a second-order Goldstone calculation of the same cluster,¹⁴ that perturbation theory is considerably improved when the Green function is used through the Dyson equation. The same range of validity is obtained by further checks that we have done for smaller clusters.

Figure 4 shows again second-order results for the ground-state energy but now obtained as a function of band filling for the largest cluster that has been studied within this total energy context (20×20 sites). Maximum filling is 0.96 in this case. In the absence of exact results for this situation we have chosen the unrestricted Hartree-Fock (UHF) method²⁷ to compare with. Results are given in panel (b) of Fig. 4. It can be shown that perturbative results are sensibly better in the whole range of filling ratios. It is interesting to notice that the relative error of the UHF calculation increases for the largest U value ($U = 6t$), in spite of being a variational approach that is valid for *large* U values. Of course, perturbation theory breaks completely down for very large interaction parameter whereas UHF theory remains being qualitatively valid even in this range.

Figure 5 shows the momentum distribution for a 20×20 cluster close to half-filling ($n = 0.96$) corresponding to three U values ($U/t = 0, 1, 4$). The distribution is given along the direction from $(0, 0)$ to (π, π) . Nothing can be said about the existence or not of a discontinuity that would define the interacting Fermi surface because the separation between points in the \mathbf{k} space is too large compared to the region where the momentum distribution drops to a small value. Nevertheless, the shape of the momentum distribution remains steplike for the studied U values, and similar to the noninteracting one, in agreement with Monte Carlo results.¹¹ Therefore, any

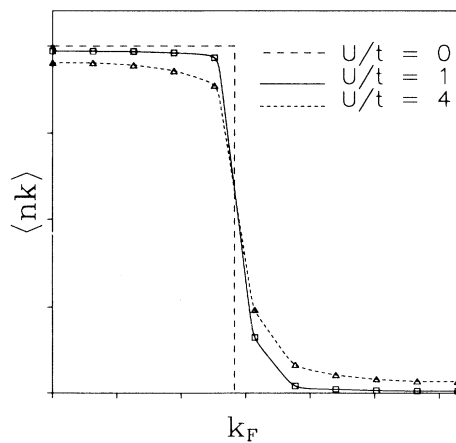


FIG. 5. Momentum distribution corresponding to the two-dimensional Hubbard model calculated for three U values by means of Eq. (6). It starts at the center of the Brillouin zone and ends at its corner. Symbols give occupation at \mathbf{k} points that actually appear in our cluster calculation whereas solid lines are simple guides for the eye.

experimental probe that tests the Fermi surface with a finite resolution would find a sharp change in $n_{\mathbf{k}}$ close to the noninteracting Fermi surface.

A very visual means to have an idea of the importance of many-body effects is just to look at the evolution of the one-body Green function as the value of the interaction parameter U increases. Figure 6 gives the imaginary part of the Green function (the spectral part) for three different values of U . It can be observed that for $U = 8t$ the interaction produces a large spreading of the spectral function of an electron at the Fermi surface. The decrease of the weight of the δ peak at the one-electron energy is related to the renormalization constant Z . The study of Z allows the characterization of the small energy excitations prevailing in the system, i.e., the physical behavior of the system. In particular, it allows the distinction between Fermi liquid and *marginal* Fermi or Luttinger liquid. In order to explore the possibility of a non-Fermi-liquid behavior of the system we have plotted the renormalization factor Z against filling for different values of the interaction and different sizes of the cluster. Results are given in Fig. 7. We find a clear nonconventional behavior when half-filling is approached. This effect is more pronounced for high values of U/t . It is worth to mentioning here that results pointing to the same kind of nonconventional behavior have been obtained within a nonhomogeneous unrestricted Hartree-Fock theory:²⁸ In this work the overlap within the UHF wave function of the half-filled system and the self-consistent ground-state wave function after the introduction of a single hole has been shown to vanish in the thermodynamic limit. Z values obtained in Ref. 28 are compatible with the second-order perturbation results of the present work.

The same nonconventional behavior of Z can also be inferred from the imaginary part of the self-energy. Figure 8 shows the imaginary part of the second-order self-energy for ω close to the Fermi energy for the largest cluster that we have studied (40×40). Ten different band fillings have been considered for an interaction energy of $U = 2t$. (Notice however that the value of U is irrelevant in a discussion of the *shape* of the second-order

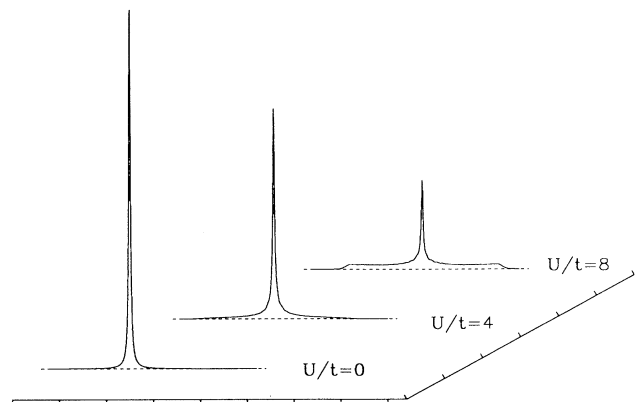


FIG. 6. Evolution of the imaginary part of the Green function at the Fermi wave vector as the value of U increases. The separation of ticks in the horizontal energy scale is $0.5t$.

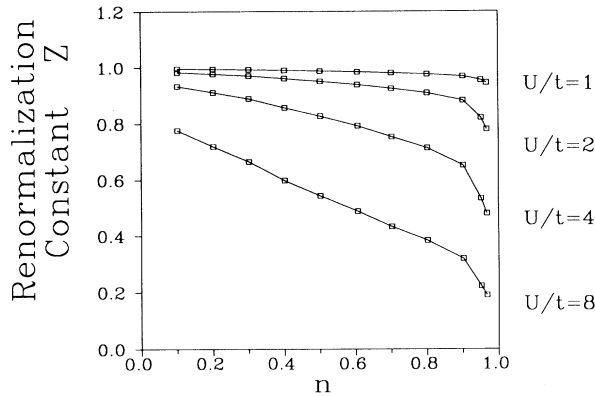


FIG. 7. Renormalization factor Z of the two-dimensional Hubbard model as a function of band filling. Several U values have been considered.

self-energy: The U^2 prefactor modifies absolute values but not forms). A linear $|\omega|$ dependence of the self-energy can be observed for fillings close to one electron per site. This very peculiar behavior disappears when the number of holes increases. A clear $|\omega|^2$ dependence is reached at a filling $n \sim 0.70$. It can be said that a gradual transition from a marginal Fermi liquid behavior to a conventional one is obtained by our perturbative analysis. This result reinforces the idea obtained from the study of Z (see Fig. 7) that although the system is strictly nonconventional at half-filling—in agreement with previous perturbative studies⁶—a *smooth* disappearance of this behavior occurs after doping. As shown by our calculation, a clear Fermi liquid situation is only reached below $n \sim 0.70$.

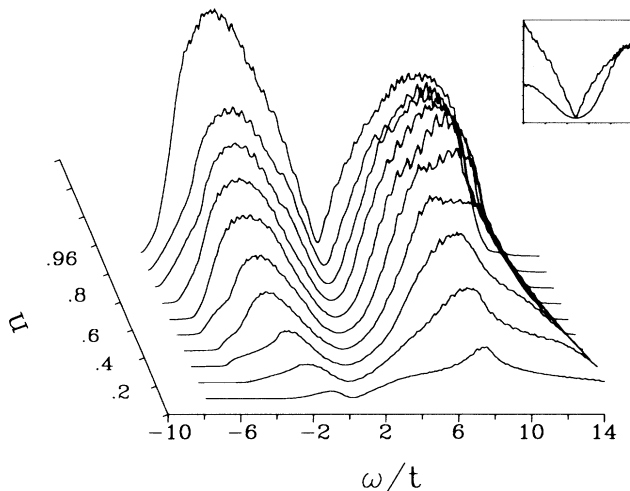


FIG. 8. Imaginary part of the second-order self-energy [see Eq. (3)] plotted as a function of ω for several band fillings. The inset gives a more quantitative comparison of the two quite different behaviors obtained: The quasilinear ω dependence obtained near half-filling changes to the standard quadratic dependence for a dilute system. The jagged behavior of the curve is due to the finite size of the cluster (40×40). We have introduced a small broadening to the δ peaks ($\eta \sim 0.02$).

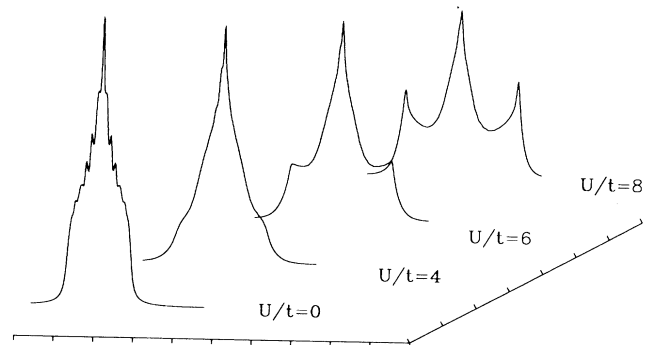


FIG. 9. Density of states as a function of ω for several U values. The system is very close to half-filling. The separation of ticks in the horizontal energy scale is $0.5t$.

The last figures (Figs. 9 and 10) show the evolution of the total density of states as U increases from 0 to $8t$. Figure 9 corresponds to a half-filled situation. It can be observed how the starting density of states showing one single central peak evolves to a three-peak shape due to the appearance of two new peaks that extend the one-particle spectrum. These peaks due to many-body effects tend to appear at $-U/2$ and $U/2$ energies for large enough U values. Figure 10 shows the same evolution but now for a cluster containing half an electron per site (one-quarter filling). Surprisingly, a new peak evolves just at the Fermi energy in a region that is initially structureless. Larger U values give rise to the standard two peak situation corresponding to the infinite U limit of the Hubbard model.

IV. CONCLUSIONS

The conclusions of our work are the following.

(i) The second-order self-energy is a good approach to the study of the Hubbard Hamiltonian for all fillings

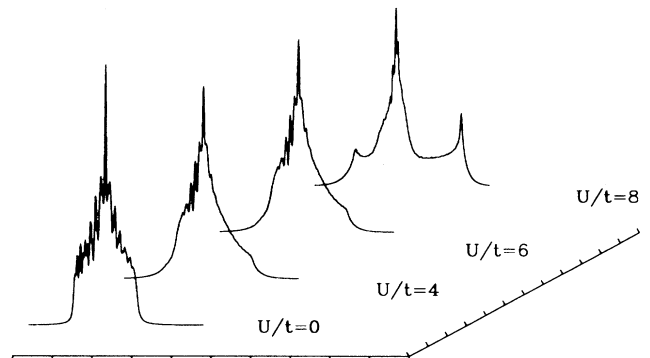


FIG. 10. Density of states as a function of ω for several U values. The filling of the system is close to one-fourth. The Fermi energy coincides with the position of the central peak. The separation of ticks in the horizontal energy scale is $0.5t$.

given that the value of the on-site interaction is not larger than the bandwidth of the noninteracting spectrum.

(ii) The Luttinger character of the one-dimensional Hubbard model manifests itself giving rise to a linear $|\omega|$ dependence of the imaginary part of the second-order self-energy. This behavior is independent of the band filling.

(iii) No matter how small is the value of U , we obtain a nonconventional behavior for the self-energy close to the Fermi energy when the half-filled situation is approached on the square lattice.

(iv) The linear $|\omega|$ dependence mentioned in the last two remarks is not restricted to the neighborhood of the Fermi energy but extends over a broad energy range (several units of t). Analytical reasons have been given to explain this property.

(v) Perturbation theory shows that although the renormalization constant Z does not vanish away from the

perfect nesting condition, its actual value is considerably smaller than one.

(vi) In our opinion, second-order perturbation theory applies to the actual interaction strengths observed in cuprate oxides. Nevertheless, a definite conclusion about the validity of perturbation theory for real materials has to wait to a future work that starts from a realistic model of the band structure of cuprate oxides.

ACKNOWLEDGMENTS

This work has been supported by the Comisión Interministerial de Ciencia y Tecnología of Spain under Contract No. MAT91-0905-C02. The authors are indebted to F. Guinea and E. Louis for stimulating discussions during the course of this work.

-
- ¹ J. G. Bednorz and K. A. Müller, *Z. Phys. B* **64**, 189 (1986).
² P. W. Anderson, *Science* **235**, 1196 (1987).
³ J. Hubbard, *Proc. R. Soc. London, Ser. A* **276**, 238 (1963); J. Kanamori, *Prog. Theor. Phys.* **30**, 275 (1963); M. C. Gutzwiller, *Phys. Rev. Lett.* **10**, 159 (1963).
⁴ *Physical Properties of High Temperature Superconductors I*, edited by D. M. Ginsberg (World Scientific, Singapore, 1989); *Physical Properties of High Temperature Superconductors II*, edited by D. M. Ginsberg (World Scientific, Singapore, 1990).
⁵ C. M. Varma, P. B. Littlewood, S. Schmitt-Rink, E. Abrahams, and A. E. Ruckenstein, *Phys. Rev. Lett.* **63**, 1996 (1989).
⁶ H. Schweitzer and G. Czycholl, *Z. Phys. B* **83**, 93 (1991).
⁷ A. Virosztek and J. Ruvalds, *Phys. Rev. B* **42**, 4064 (1990).
⁸ P. A. Lee and N. Read, *Phys. Rev. Lett.* **25**, 2691 (1987).
⁹ B. R. Alascio and C. R. Proetto, *Solid State Commun.* **75**, 217 (1990).
¹⁰ E. Müller-Hartmann, *Z. Phys. B* **74**, 507 (1989); **76**, 211 (1989).
¹¹ A. Moreo, D. J. Scalapino, R. L. Sugar, S. R. White, and N. E. Bickers, *Phys. Rev. B* **41**, 2313 (1990).
¹² E. Louis, F. Flores, C. Tejedor, and A. Martín-Rodero, *Phys. Rev. B* **30**, 7299 (1984); **33**, 1814 (1986); M. M. Steiner, R. C. Albers, D. J. Scalapino, and L. J. Sham, *ibid.* **43**, 1637 (1991); H. Schweitzer and G. Czycholl, *Phys. Rev. Lett.* **67**, 3724 (1991).
¹³ N. Bulut and D. J. Scalapino, *Phys. Rev. Lett.* **67**, 2898 (1991); **68**, 706 (1992).
¹⁴ J. Galán and J. A. Vergés, *Phys. Rev. B* **44**, 10 093 (1991).
¹⁵ A. M. Oleś, G. Tréglia, D. Spanjaard, and R. Jullien, *Phys. Rev. B* **32**, 2167 (1985).
¹⁶ A. A. Abrikosov, L. P. Gorkov, and I. E. Dzyaloshinski, *Methods of Quantum Field Theory in Statistical Physics* (Prentice-Hall, Englewood Cliffs, 1964).
¹⁷ B. Friedman, *Europhys. Lett.* **14**, 495 (1991).
¹⁸ W. Metzner and D. Vollhardt, *Phys. Rev. B* **39**, 4462 (1989); *Phys. Rev. Lett.* **62**, 324 (1989).
¹⁹ G. Dopf, A. Muramatsu, and W. Hanke, *Phys. Rev. Lett.* **68**, 353 (1992).
²⁰ P. W. Anderson (unpublished).
²¹ P. W. Anderson, *Phys. Rev. Lett.* **64**, 1839 (1990); **65**, 2306 (1990).
²² J. M. Luttinger, *Phys. Rev.* **121**, 942 (1961).
²³ H. Shiba, *Phys. Rev. B* **6**, 930 (1972).
²⁴ J. E. Hirsch and S. Tang, *Phys. Rev. B* **31**, 4403 (1985); *Phys. Rev. Lett.* **62**, 591 (1989); J. Bonca, P. Prelovšek, and I. Sega, *Phys. Rev. B* **39**, 7074 (1989); S. R. White, D. J. Scalapino, R. L. Sugar, E. Y. Loh, J. E. Gubernatis, and R. T. Scalettar, *ibid.* **40**, 506 (1989); E. Dagotto, A. Moreo, R. L. Sugar, and D. Touissant, *ibid.* **41**, 811 (1990).
²⁵ A. Parola, S. Sorella, S. Baroni, M. Parrinello, and E. Tosatti, *Int. J. Mod. Phys. B* **3**, 1865 (1989); G. Fano, F. Ortolani, and A. Parola, *Phys. Rev. B* **42**, 6877 (1990).
²⁶ E. Dagotto, A. Moreo, F. Ortolani, D. Poilblanc, and J. Riera, *Phys. Rev. B* **45**, 10741 (1992).
²⁷ A. R. Bishop, F. Guinea, P. S. Lomdahl, E. Louis, and J. A. Vergés, *Europhys. Lett.* **14**, 157 (1991); J. A. Vergés, E. Louis, P. S. Lomdahl, F. Guinea, and A. R. Bishop, *Phys. Rev. B* **43**, 6099 (1991); F. Guinea, E. Louis, and J. A. Vergés, *ibid.* **45**, 4752 (1992); *Europhys. Lett.* **17**, 455 (1992); E. Louis, J. Galán, F. Guinea, J. A. Vergés, and J. Ferrer, *Phys. Status Solidi B* **173**, 715 (1992).
²⁸ J. Galán, F. Guinea, J. A. Vergés, G. Chiappe, and E. Louis, *Phys. Rev. B* **46**, 3163 (1992).